Journal of the Geological Society, London, Vol. **157**, 2000, pp. 367–379. Printed in Great Britain.

An oxygen and carbon isotopic study of multiple episodes of fluid flow in the Dalradian and Highland Border Complex, Stonehaven, Scotland

R. L. MASTERS, J. J. AGUE & D. M. RYE

Yale University, PO Box 208109, New Haven, CT 06520-8109, USA (e-mail: masters@hess.geology.yale.edu)

Abstract: The carbon and oxygen systematics of rocks north of Stonehaven, Scotland were studied to provide new constraints on the nature and timing of metamorphic and post-metamorphic fluid infiltration. Carbon and oxygen isotopic data were collected from carbonated spilites and carbonate-bearing veins in the Highland Boundary Fault, from Dalradian metacarbonate layers and pervasively carbonated schists, and from three generations of carbonate-bearing veins, and a quartz porphyry dyke within the Dalradian. Isotopic evidence for syn-metamorphic fluid infiltration in the Dalradian is preserved in quartz–calcite veins in the upper chlorite zone and in staurolite zone metacarbonates. $\delta^{18}O$ values for coexisting quartz ($\delta^{18}O_{quartz}=13.6‰$) and calcite ($\delta^{18}O_{calcite}=11.6‰$) in a vein from the upper chlorite zone are consistent with precipitation of both minerals from a single fluid at *c.* 375°C. Oxygen isotopic data from staurolite zone metacarbonate layers ($\delta^{18}O_{calcite}=10.4$ to 12.9‰) suggest major isotopic exchange with an external fluid equilibrated with a quartzo-feldspathic reservoir, such as the Dalradian metasediments, at metamorphic temperatures. Low, negative carbon isotope data from these metacarbonate layers ($\delta^{13}C_{calcite}=-12.4$ to $-17.7‰$) may indicate a component of oxidized organic material in the infiltrating fluid. Post-metamorphic fluids derived from or equilibrated with a high-temperature silicate reservoir such as felsic igneous rocks were responsible for precipitation of post-metamorphic vein carbonate, carbonation of pelitic schists, and alteration of metamorphic feldspar porphyroblasts from Barrow's famous spotted chloritoid schists in an area geographically associated with several carbonated quartz porphyry dykes. Some veins in the biotite and garnet zones have been conduits for multiple generations of fluid flow. Quartz from this generation of veins preserves a metamorphic isotopic signature ($\delta^{18}O_{quartz}=11.2$ to 13.2‰) whereas dolomite and calcite are considered to be post-metamorphic based on textural evidence and isotopic data indicating extreme oxygen isotopic disequilibrium between vein quartz and carbonate minerals ($\delta^{18}O_{dolomite}=23.7$ to 24.2‰, $\delta^{18}O_{calcite}=25.3‰$, $\delta^{18}O_{quartz}=11.2$ to 13.2‰). Variably depleted carbon isotopes from carbonate minerals in these veins ($\delta^{13}C_{dolomite}=-8.1$ to $-13.4‰$, $\delta^{13}C_{calcite}=-12.2‰$) may reflect input of oxidized organic material in the mineralizing fluid. Isotopic data from carbonate veins and variably carbonated spilites from the Highland Boundary Fault are consistent with hydrothermal alteration of basalts by seawater, which had its carbon isotope systematics modified by addition of magmatic CO_2 and/or oxidation of organic carbon. Such alteration may have occurred on the seafloor or during emplacement in the Highland Boundary Fault.

Keywords: Dalradian, Highland Boundary Fault, Stonehaven Scotland, ^{13}C, ^{18}O.

The area just north of Stonehaven, Scotland, is ideal for studying the effects of fluid-rock interaction in diverse geological settings (Fig. 1). Here, there is nearly 100% exposure of key structures and rock packages involved in the crustal development of Scotland including the Highland Boundary Fault, the intensely folded and boudinaged pelitic and psammitic sediments of the Southern Highland Group of the Dalradian, syn- and post-metamorphic vein arrays in both the Highland Boundary Fault and the Dalradian metasediments, and post-metamorphic quartz porphyry dykes.

We present the first study of the oxygen and carbon isotope systematics of carbonate minerals and vein quartz from the Stonehaven area to provide a more complete understanding of fluid reservoirs and timing of fluid infiltration affecting the Highland Boundary Fault, the Dalradian metasediments, and the quartz porphyry intrusions. We constrain (1) possible fluid reservoirs including magmatic, metamorphic, and surface fluids; (2) the temperature ranges of isotopic alteration; and (3) the relative timing of fluid infiltration and tectono-metamorphic events including regional metamorphism, dyke intrusion, and crustal-scale faulting. Identification of potential fluid reservoirs and timing of different episodes of fluid infiltration helps characterize environments of fluid–rock interaction through time.

Regional geology

Dalradian metasediments

The Dalradian metasediments are a series of pelites, psammites, and limestones (Harris & Pitcher 1975) that were deposited in a marginal basin environment on the Laurentian continent (Fettes *et al.* 1986). Our study area is within the stratigraphically highest metasediments, the Southern Highland Group, whose protoliths were a succession of turbidite facies psammitic and pelitic sediments that include rare sedimentary carbonate layers.

Barrovian metamorphism of the Dalradian metasediments occurred during the Grampian Orogeny at 500–490 Ma (Fettes 1979; Rogers *et al.* 1989). Metamorphic grade increases from greenschist facies near the Highland Boundary Fault to amphibolite facies northwest of the fault. Pressure ranges from 3–5 kbar in northeastern Scotland near Stonehaven (Droop &

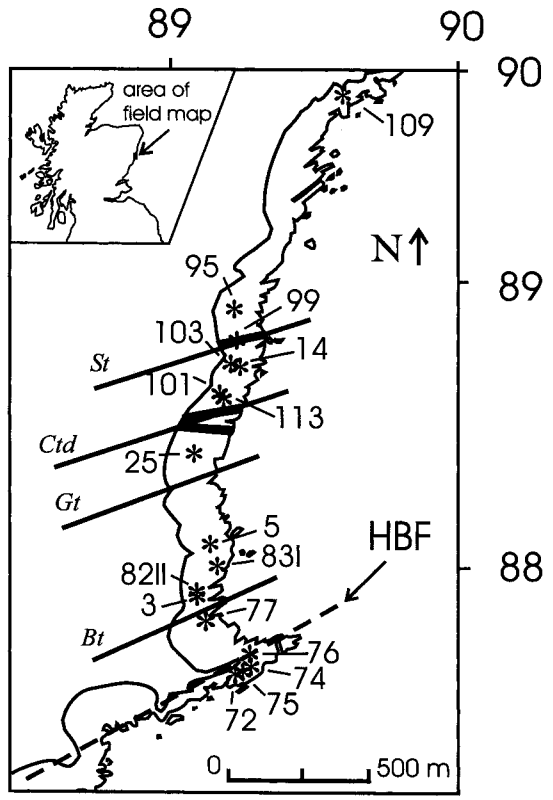

Fig. 1. Map of field area. Inset shows location of field map in northeastern Scotland. Asterisks (*) denote sample locations. The sample number prefix JAB has been omitted for clarity. Light solid lines denote extent of coastal exposure, defined on the west by the base of the seacliff and on the east by the low tide limit (British Geological Survey, 1:50 000 map series, Scotland Sheet 67). Heavy dashed line denotes trace of Highland Boundary Fault (HBF). Heavy solid lines indicate the biotite (Bt), garnet (Gt), chloritoid (Ctd), and staurolite (St) isograd locations based on Barrow (1912), Droop and Harte (1995) and our field study. Quartz porphyry dikes are shown in grey. Sample location JAB 15 (not shown) is located on the coastline about 4 km north of the HBF (^{3}90.3 m. E., ^{7}91.6 m. N.), near the town of Muchalls. Co-ordinates correspond to the National Grid system, sheet NO.

Harte 1995; Ague 1997) to 8–10 kbar in the central and southwest Highlands (Harte 1988; Skelton *et al.* 1995).

The Dalradian metasediments of Scotland and Ireland are among the most extensively studied metamorphic rocks in the world. Pioneering work in the study of index mineral development (Barrow 1893; Tilley 1925) and the relationship between pressure, temperature, and metamorphic isograds (Tilley 1924; Chinner 1966) was begun in the Dalradian. More recent work has shown that fluid flow was integral to regional metamorphic and post-metamorphic processes in the Dalradian (Graham *et al.* 1983; Craw 1990; Jenkin *et al.* 1992; Cole & Graham 1994; Fein *et al.* 1994; Skelton *et al.* 1995; Ague 1997). Dalradian metasediments contain abundant vein arrays. Some veins formed by silica diffusion from local wall rock into fractures during metamorphism and probably transmitted little fluid (e.g. Yardley & Bottrell 1992). Other veins, however, almost certainly represent conduits for regional-scale fluid flow (Craw 1990; Ague 1997; Graham *et al.* 1997).

Four Grampian deformational events affected the Dalradian, forming and refolding major nappe structures (Shackleton 1958; Harris *et al.* 1976). The first three deformational events (D1–D3) occurred during regional Barrovian metamorphism of the Dalradian metasediments; peak temperatures were reached during D3 (Harte *et al.* 1984). A post peak-metamorphic deformation event (D4) is thought to have formed a downbend of the regional nappe structures along a basement fault parallel to and possibly related to the Highland Boundary Fault. The creation of two structural provinces in the Dalradian has been attributed to D4; the Highland Border Steep Belt, a zone near the Highland Boundary Fault where regional structures are steeply dipping, and the Flat Belt, beginning *c.* 5–15 km north of the Highland Boundary Fault (Harte *et al.* 1984).

Within the Highland Border Steep Belt, our field area includes *c.* 2 km of continuous coastal exposure (Fig. 1). One additional site, not shown on Fig. 1, is located within the Flat Belt, *c.* 4 km north of the Highland Boundary Fault. Metamorphic grade increases northward from the Highland Boundary Fault, through the eastward extension of Barrow's chlorite, biotite, garnet, and staurolite zones (Fig. 1; Barrow 1912; Atherton 1977; Yardley & Baltatzis 1985; Droop & Harte 1995).

Highland Boundary Fault

The Highland Boundary Fault is a major tectonic boundary that has been traced east to west across the width of Scotland and Ireland. In Scotland, the Highland Boundary Fault divides the Devonian metasediments of the Midland Valley Terrane from the Precambrian to Cambrian metasediments of the Grampian Terrane to the north. It has been recognized for decades that the Highland Boundary Fault has played an important role in the tectonic development of Scotland (Anderson 1947; Henderson & Robertson 1982; Harte *et al.* 1984; Hutton 1987; Ryan *et al.* 1995), but the nature of that role is not yet completely resolved (cf. Tanner 1995).

Embedded within the Highland Boundary Fault are slivers of a dismembered ophiolite and associated sediments called the Highland Border Complex (Henderson & Robertson 1982). At Stonehaven, the Highland Border Complex includes fault-bounded blocks of both igneous and sedimentary rocks. Igneous rocks in our field area include spilitized pillow lavas and serpentinites metamorphosed to greenschist facies (Ikin & Harmon 1983). Carbonate alteration and veining is widespread. Interlava sediments include metamorphosed siltstone, mudstone and iron-rich chert. Cherts are interpreted as hydrothermal precipitates whereas siltstone and mudstone layers are likely distal turbidite deposits of terriginous sediments from a source similar to the Dalradian metasediments (Robertson & Henderson 1984). Tanner (1995), working in the Keltie Water Grit Formation at Callander, concluded that the metasediments of the Highland Border Complex and the upper Dalradian form a continuous sedimentary sequence that has undergone the same deformation history. Hydrogen and oxygen isotope systematics of silicates from the Highland Border Complex at several locations along the length of the Highland Boundary Fault suggest near-surface exchange with meteoric fluids as well as greenschist facies metamorphism accompanied by exchange with Dalradian metamorphic fluids (Ikin & Harmon 1983).

Post-metamorphic igneous rocks

Quartz porphyry dykes, also called felsite dykes, intruded the Dalradian metasediments exposed just north of Stonehaven

(British Geological Survey 1:50 000 series, Scotland Sheet 67). These dykes intruded during the late stages of the Caledonian Orogeny and are believed to be genetically associated with the Younger Granite Series (*c.* 400–460 Ma, Munro 1986). Dykes of this type are common throughout the Southern Highland Group of the Dalradian and range in length from tens to hundreds of metres (British Geological Survey, 1:50 000 series).

The dykes outcrop within metasediments severely altered due to retrograde processes in the Stonehaven area (Chinner 1967; Yardley & Baltatzis 1985). At least some of this retrogression may be genetically linked to the intrusion of the dykes. Many studies have shown that igneous intrusions may drive hydrothermal fluid circulation that has the potential to alter both the stable isotope systematics and the mineralogy of the country rock (Taylor 1974).

Methods

Sample preparation

Carbonate mineralogy was determined at Yale University using either a Scintag PAD V X-ray diffractometer or energy-dispersive spectrometry on the JEOL JXA-8600 electron microprobe.

High spatial resolution (mm scale) sampling of carbonate minerals in spots, veinlets, and veins was done using a dental drill equipped with a 0.5 mm diameter diamond-tipped bit. All other carbonate samples were obtained from bulk samples of the rocks that were ground into a fine powder using an agate mortar and pestle and then sieved to obtain a uniform size fraction between 180 and 250 μm.

Carbonate samples were reacted with 100% orthophosphoric acid by two methods at 90°C. Samples were either reacted individually in a common acid bath (CAB) following the method described by Swart *et al.* (1991), or they were reacted in individual sealed vessels. Several samples were run using both methods and the results for these samples were indistinguishable within analytical error. Gas extracted from samples containing sulphides was reacted with silver phosphate to remove H_2S.

Quartz collected from veins was crushed and hand picked under a binocular microscope. The purified fraction was then ground in an agate mortar and sieved to obtain a uniform size fraction between 180 and 250 μm. Oxygen extraction, performed on a standard BrF_5 extraction line following the method of Clayton & Mayeda (1963), produced CO_2 for oxygen isotope analysis.

Isotope analysis

Isotope ratios from both carbonate and quartz-derived carbon dioxide were analysed using a Finnigan Mat 251 EM mass spectrometer at Yale University. Carbon and oxygen isotope ratios for our samples are reported in standard δ notation relative to PDB and V-SMOW respectively (Tables 1 and 2). Laboratory precision for carbonate samples was evaluated using replicate analyses of a laboratory calcite standard with $\delta^{18}O = 19.7 \pm 0.13‰$ (1σ standard deviation) and $\delta^{13}C = 1.1 \pm 0.06‰$ (1σ standard deviation). Laboratory precision for quartz was evaluated using a laboratory quartz standard with $\delta^{18}O = 12.6 \pm 0.17‰$ (1σ standard deviation). We report $\delta^{18}O_{V\text{-}SMOW} = 9.7 \pm 0.21$ for National Bureau of Standards (NBS) 28, quartz standard, and a value of $\delta^{18}O_{PDB} = -2.7 \pm 0.07$ (1σ standard deviation) and $\delta^{13}C_{PDB} = 2.0. \pm 0.01$ (1σ standard deviation) for NBS 19, calcite standard.

Metacarbonate mineral chemistry

Mineral rim compositions from staurolite zone metacarbonate layers were determined using wavelength dispersive spectrometry on the JEOL JXA-8600 electron microprobe at Yale University (Table 3). Accelerating voltage and beam current were 15 kV and 20 nA, respectively, for all minerals except calcite where a beam current of 10 nA was used. Off-peak background corrections were used for all elements. Matrix corrections (φ–ρ–*z*) for calcite and clinozoisite specified three oxygens per carbon atom and 13 oxygens per hydrogen atom respectively.

Samples and isotopic results

Samples were gathered from (1) carbonate veins and variably carbonated spilites from the Highland Boundary Fault, (2) metacarbonate layers and concretion lenses, carbonate veins, carbonate-bearing quartz veins and pervasively carbonated schists from the Dalradian metasediments, and (3) carbonate-bearing alteration of a quartz porphyry dyke (Fig. 1, Table 1). Quartz was collected from several carbonate-bearing quartz veins within the Dalradian (Table 2).

Highland Boundary Fault

Carbonate minerals in the Highland Boundary Fault are found in pervasive alteration and crosscutting veins within the spilitized basalt. Calcite veins within spilites are highly deformed and range in width from a few millimetres to *c.* 2 cm. Spilites also contain chlorite, albite, quartz and pyrite. In some areas, vein-bearing spilites grade over the centimetre to metre scale into pervasively dolomitized rock consisting of quartz, dolomite, kaolinite and pyrite. Pervasively dolomitized rocks sometimes preserve foliation present in less altered spilites and contain kaolinite and carbonate minerals pseudomorphic after plagioclase laths (Fig. 2). Massive, pink ferruginous dolomite is also found in veins from tens of centimetres up to several metres wide (referred to as a 'dyke-like mass' in the British Geological Survey 1:50 000 map series, Scotland Sheet 67), crosscutting fault-bounded blocks of spilite and associated sediments. Ferruginous dolomite veins host thin (*c.* 0.5–1 cm) cross-cutting veinlets containing euhedral dolomite crystals characterized by oscillatory zoning between dolomite and ferruginous dolomite (Fig. 3a). Dolomite is also found in vugs within the ferruginous dolomite veins.

Isotopic data from Highland Boundary Fault rocks, including wholerock samples of dolomitized spilites, spilites with abundant millimetre-thick calcite veinlets, a ferruginous dolomite vein, and a dolomite-bearing veinlet define a data array with a positive slope on a $\delta^{13}C$ versus $\delta^{18}O$ diagram (Fig. 4). The $\delta^{13}C$ for most samples ranges from 0.2 to $-5.2‰$ and the $\delta^{18}O$ ranges from 14.9 to 20.1‰. Sample JAB 75A-1, from a 2–3 cm wide calcite vein within spilitic rock, has a somewhat lower $\delta^{18}O = 11.4‰$ with $\delta^{13}C = -1.7‰$.

Porphyry dykes

Three quartz porphyry dykes intrude the Dalradian metasediments within the study area and are roughly concordant with the strike of regional foliation. The dykes have been heavily altered to quartz, sericite, kaolinite, dolomite, and pyrite, but the original porphyritic texture of the rocks is commonly preserved. For example, kaolinite ± dolomite pseudomorphs after plagioclase phenocrysts are common. Dolomite is also disseminated through the rock matrix. Dolomite from one of the porphyry dykes (JAB 99A) has $\delta^{18}O = 22.5‰$ and $\delta^{13}C = -3.1‰$ (Fig. 5).

Pervasive carbonation

A broad region of red-weathering, pervasively carbonated schists surrounds the dykes. Other locations along the coast

Table 1. *Data from Highland Boundary Fault and Dalradian carbonate*

Sample*	Zone	Distance from HBF (m)	Type	$\delta^{18}O$	$\delta^{13}C$	Carbonate
JAB 72A-1†	HBF	0	Vein	19.1	0.27	Fe-dolomite
				19.2	0.15	
JAB 72A-2†	HBF	0	Carbonated spillite	20.0	−1.14	Fe-dolomite
				20.1	−1.33	
				20.1	−1.30	
JAB 72A-3†	HBF	0	Vein	19.2	−0.67	Dolomite
JAB 72B	HBF	0	Carbonated spillite	18.3	−1.41	Dolomite
JAB 74A	HBF	0	Veined spillite	14.9	−3.45	Calcite
JAB 75A-1	HBF	0	Vein	11.3	−1.67	Calcite
				11.5	−1.69	
JAB 75A-2	HBF	0	Veined spillite	17.5	−4.05	Calcite
JAB 76A†	HBF	0	Carbonated spillite	17.5	−3.13	Fe-dolomite
				17.5	−3.22	
JAB 76B	HBF	0	Veined spillite	15.0	−5.20	Calcite
JAB 77A-1	Chlorite	183	Vein type B	11.5	−8.96	Calcite
				11.6	−8.95	
JAB 77A-2	Chlorite	183	Vein type B	14.5	−5.85	Calcite
				13.4	−5.90	
JAB 3A‡	Biotite	279	Vein type A	23.7	−13.40	Dolomite
				23.8	−12.87	
				23.9	−12.24	
				23.9	−12.00	
				24.2	−12.74	
				24.2	−12.16	
JAB 3D	Biotite	279	Pervasive carbonation	22.4	−5.45	Siderite
JAB 3E	Biotite	279	Concretion lens	23.4	−6.02	Fe-dolomite
JAB 82II1G	Biotite	294	Vein type A	24.0	−8.07	Dolomite
JAB 83IA-1‡	Biotite	328	Vein type C	18.3	−4.18	Fe-dolomite
				17.9	−3.86	
JAB 83IA-2	Biotite	328	Veintype C	18.2	−4.80	Dolomite
JAB 5A	Biotite	423	Vein type A	24.1	−4.40	Dolomite
JAB 5D	Biotite	423	Pervasive carbonation	20.8	−5.11	Siderite
JAB 25A	Garnet	747	Concretion lens	23.8	−11.34	Dolomite
				23.8	−11.34	
JAB 25C	Garnet	747	Vein type C	25.2	−5.75	Dolomite
JAB 113C	Chloritoid	887	Vein type A	25.3	−12.37	Calcite
				25.2	−11.99	
JAB 101A‡	Chloritoid	903	Spot	28.0	−19.9	Calcite
				27.0	−1.96	
JAB 101J‡	Chloritoid	903	Spot	22.0	−57.6	Calcite
				23.1	−5.31	
				23.2	−4.87	
JAB 14H	Chloritoid	919	Spot	24.0	−5.25	Calcite
JAB 103A	Chloritoid	982	Spot	20.2	−6.22	Calcite
JAB 99A	Staurolite	1055	Porphyry dyke	22.5	−3.13	Dolomite
JAB 95B	Staurolite	1167	Spot	22.1	−4.45	Calcite
JAB 109F	Staurolite	1712	Marble	11.1	−16.86	Calcite
				10.7	−17.66	
				10.4	−17.71	
JAB 15B-1	Staurolite	~3000	Marble	12.2	−13.81	Calcite
JAB 15B-2	Staurolite	~3000	Marble	12.0	−13.35	Calcite
				12.7	−12.38	

*See Fig. 1 for sample locations.
†Denotes samples from 'dyke-like mass' described in British Geological Survey 1:50 000, Scotland Sheet 67.
‡Multiple analyses represent individual powder samples from closely spaced (mm scale) sites in the hand specimen. All other multiple analyses represent repeat analyses of the same powder.

show evidence of this 'reddening', with or without carbonation. Based on reconnaissance mapping, the area immediately surrounding the quartz porphyry dykes appears to have the most extreme carbonate alteration. Sulphides, including pyrite and chalcopyrite, are ubiquitous in rocks with this type of alteration and are probably responsible, at least in part, for the red weathering. Fresh, unweathered rock is light greenish-grey beneath the red weathering rinds. Samples were collected from pervasively carbonated schists as well as carbonate from carbonate-bearing veins within these 'red zones'. The most highly altered rocks contain quartz, muscovite, disseminated siderite or ferruginous dolomite and kaolinite with lesser

Table 2. *Data from Dalradian vein quartz*

Sample*	Zone	Distance from HBF (m)	Type	$\delta^{18}O$ (‰)
JAB 77A	Chlorite	183	Vein type B	14.0
				13.3
JAB 3A-7	Biotite	279	Vein type A	12.2
				11.2
JAB 3A-9	Biotite	279	Vein type A	13.2
				12.0
JAB 82II1G	Biotite	294	Vein type A	12.0
				11.6

*See Fig. 1 for sample locations.
HBF, Highland Boundary Fault.

hematite, rutile, pyrite and chalcopyrite. Somewhat less altered schists that contain quartz, biotite, muscovite, tourmaline and accessory hematite, rutile, pyrite and chalcopyrite have dolomite localized along lamellae parallel to the mica foliation. Relict garnet and chloritoid are found in altered schists within their respective metamorphic zones. Two samples of carbonated schist were studied from the biotite zone. Sample JAB 5D is pervasively dolomitized (Fig. 6a), whereas, in sample JAB 3D, dolomite is concentrated in thin (<1 mm thick) veinlets parallel to schistosity (Fig. 6b). Dolomite from these schists has uniform $\delta^{13}C$ values of -5.1 and -5.4‰ and slightly more variable $\delta^{18}O$ values of 20.8 and 22.4‰ (Fig. 5).

Fig. 2. Photomicrograph using plane-polarised light of a pervasively dolomitized spilite from the Highland Border Complex (JAB 76A). Low-relief (white) rectangular and needle-like shapes are kaolinitic clay pseudomorphic after plagioclase phenocryst laths. Moderate relief (grey) minerals, shown by the arrow, are dolomite. The dark groundmass is composed of finely intergrown quartz, clay, and dolomite stained by limonite. Field of view is 1.5 mm across.

Barrow's spots

Barrow's (1898) original study of the chloritoid-bearing rocks of the Stonehaven area focused on schists with 'white or yellowish spots', which often contain chloritoid. Barrow, and later Chinner (1967), described these spots as a significant genetic feature of chloritoid-zone rocks. Chloritoid-zone spots are metamorphic plagioclase porphyroblasts, which grew over a pre-existing metamorphic fabric and that have been retrogressively altered to assemblages of sericite, kaolinite, albite and carbonate minerals (Ague 1997). Carbonate in the spots is dominantly calcite but rare dolomite ± siderite is found in some samples. Inclusions of Fe–Ti oxides and chloritoid are

Table 3. *Mineral rim analyses from staurolite zone metacarbonate layers*

	JAB 109			JAB 15		
	Garnet	Plagioclase	Calcite	Garnet	Clinozoisite	Calcite
SiO_2	37.46	58.48	0.02	38.50	38.99	0.02
TiO_2	0.13	na	na	0.06	0.03	na
Al_2O_3	20.91	26.25	na	21.57	30.49	na
FeO^T	19.12	0.15	1.10	17.33	4.42	0.57
MnO	9.45	na	0.75	8.38	0.28	0.65
MgO	0.98	na	0.50	0.90	0.03	0.26
CaO	11.50	7.71	54.06	14.59	24.10	55.01
Na_2O	na	7.19	na	na	na	na
K_2O	na	0.07	na	na	na	na
BaO	na	0.01	na	na	na	na
CO_2*	na	na	43.24	na	na	43.24
Total	99.55	99.86	99.67	101.33	98.34	99.75
(O=)	(12)	(8)	(3)	(12)	(12.5)	(3)
Si	3.000	2.617	0.000	3.004	3.137	0.001
Al	1.974	1.385	na	1.983	2.777	na
Ti	0.008	na	na	0.004	0.002	na
Fe	1.281	0.006	0.016	1.131	0.286	0.008
Mn	0.641	na	0.011	0.554	0.018	0.010
Mg	0.117	na	0.013	0.105	0.004	0.006
Ca	0.986	0.370	0.975	1.220	1.996	0.991
Na	na	0.624	na	na	na	na
K	na	0.004	na	na	na	na
Ba	na	0.000	na	na	na	na

na, not analysed.
*Calculated during matrix correction iterations.
FeO^T, all Fe as FeO.

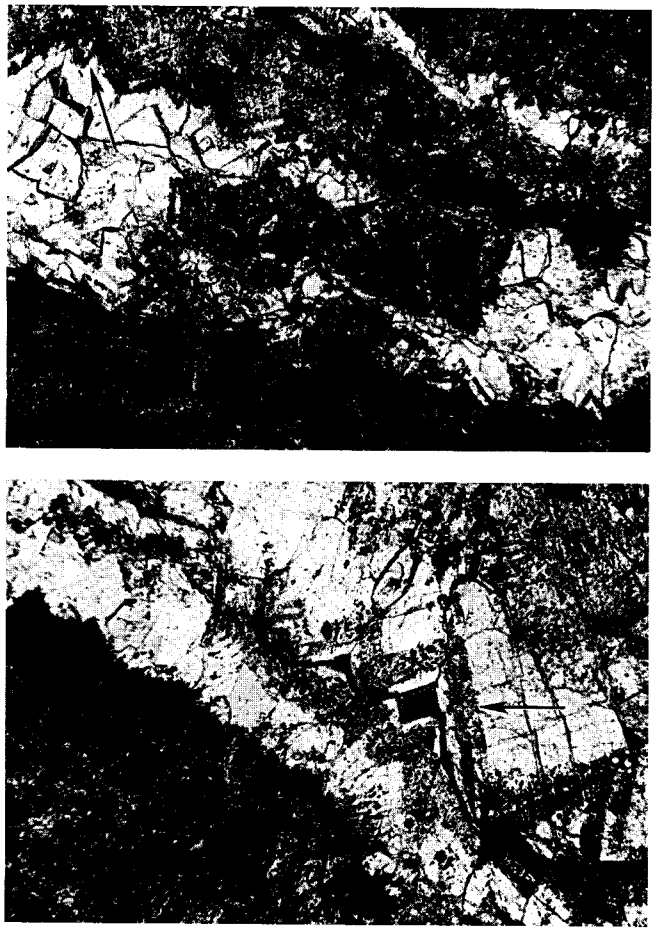

Fig. 3. Photomicrographs using plane-polarised light of zoned dolomite veins. (**a**) Vein from sample JAB 72A in the Highland Boundary Fault (HBF). Field of view is entirely of vein carbonate. Inclusion rich Fe-dolomite (dark margins) surrounds the vein centre of inclusion-free dolomite. Inclusions in the Fe-dolomite highlight euhedral growth faces (arrow), strongly suggesting that the minerals were precipitated from a fluid in an open crack. Field of view is 2.9 mm across. (**b**) Vein JAB 83IA from the Dalradian biotite zone. Major features of this vein are similar to JAB 72A from the HBF (above). Inclusion-rich Fe-dolomite, showing euhedral growth faces (arrow), bounds a vein centre of inclusion-free dolomite. Field of view is 2.9 mm across.

common in the spots and have orientations subparallel to their counterparts in the schist outside the spots. Carbonate minerals are rare or absent in the schist matrix surrounding the spots. Isotopic data from Barrow's spots defines a data array with a positive slope (Fig. 5). $\delta^{18}O$ and $\delta^{13}C$ vary from 20.1 to 28.0‰ and -2.0 to -6.2‰ respectively.

Primary carbonate minerals

Metamorphosed sedimentary carbonate rocks are rare in the Southern Highland Group within our study area. Samples were analysed from two metamorphosed concretion lenses and two metacarbonate layers.

Rare concretion lenses, 4–6 cm in long dimension, were found within the biotite zone. They consist predominantly of quartz, plagioclase and dolomite, but include minor chlorite, biotite and muscovite. Pyrite, chalcopyrite and hematite–rutile replacing magnetite are common accessory minerals. Whole-rock dolomite samples from two biotite zone concretion lenses have variable $\delta^{13}C$ (-6.0 and -11.3‰) and fairly constant $\delta^{18}O$ values (23.4 and 23.8‰) (Fig. 5).

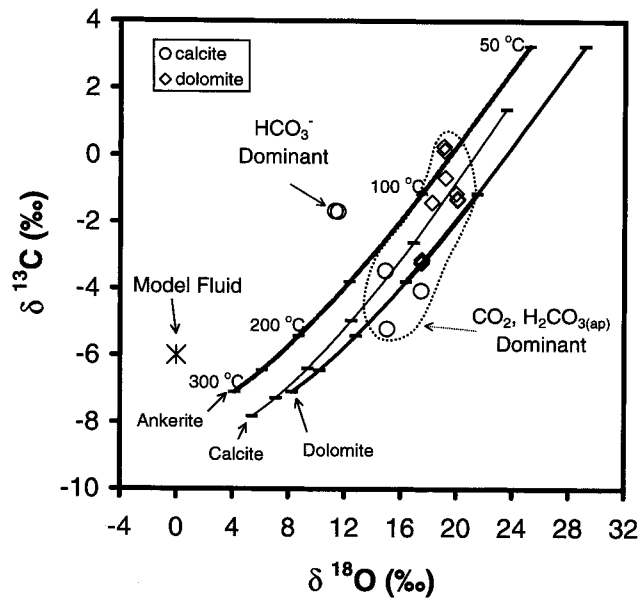

Fig. 4. $\delta^{13}C$–$\delta^{18}O$ plot of data for Highland Boundary Fault carbonates. Heavy black curve, heavy grey curve and fine black curves for dolomite, ankerite, and calcite, respectively, in equilibrium with the model fluid. Data are fit by a model for the precipitation of calcite, dolomite, or ankerite from a CO_2 or $H_2CO_{3(ap)}$-bearing fluid of constant isotopic composition ($\delta^{18}O=0$‰, $\delta^{13}C=-6$‰) over the temperature range 75–150°C. Mineral composition curves calculated using the fractionations (Δ) of Bottinga (1968) for $\Delta_{CO_2\text{-CALCITE}}$ and $\Delta_{CO_2\text{-DOLOMITE}}$, O'Neil *et al.* (1969) for $\Delta_{CALCITE\text{-}H_2O}$, Northrop & Clayton (1966) for $\Delta_{DOLOMITE\text{-}H_2O}$, and Mumin *et al.* (1996) for $\Delta_{ANKERITE\text{-}H_2O}$. Fractionations involving CO_2 were used to approximate fractionation for $H_2CO_{3(ap)}$ (see text). Outlier vein calcite composition ($\delta^{18}O=11.4$‰, $\delta^{13}C=-1.7$‰) may be due to a fluid that had HCO_3^- as the dominant carbon species (see text).

The metacarbonate layers range from *c.* 4 cm to *c.* 1 m in thickness. Both metacarbonate layers have been metamorphosed to amphibolite facies and are surrounded by staurolite-mica schists. JAB 109F is located within the Highland Border Steep Belt whereas JAB 15A is located north of the D4 downbend. Both metacarbonates have similar mineralogy, consisting of quartz, calcite, chlorite, plagioclase, and common calc-silicate minerals including garnet ± clinozoisite–epidote solid solution ± calcic amphibole. The southernmost metacarbonate layer (JAB 109F) has $\delta^{13}C_{calcite}=-17.4$‰ and $\delta^{18}O_{calcite}=10.7$‰, whereas the northernmost (JAB 15B) has $\delta^{13}C_{calcite}=-13.2$‰ and $\delta^{18}O_{calcite}=12.4$‰.

Dalradian-hosted veins

Carbonate minerals are also found within veins cutting chlorite, biotite, and garnet-zone schists. Veins can be classified into three groups (vein Types A, B, and C herein) based on their structural orientation and petrographic characteristics. Type A veins include tube-shaped quartz veins between *c.* 10 and 30 cm in thickness found within the necks of the metre-scale boudins prevalent within the section. These veins are also parallel to the axes of the metre-scale, tight to isoclinal folds that dominate the local structure. Also included in the set of Type A veins are planar quartz veins which extend from the

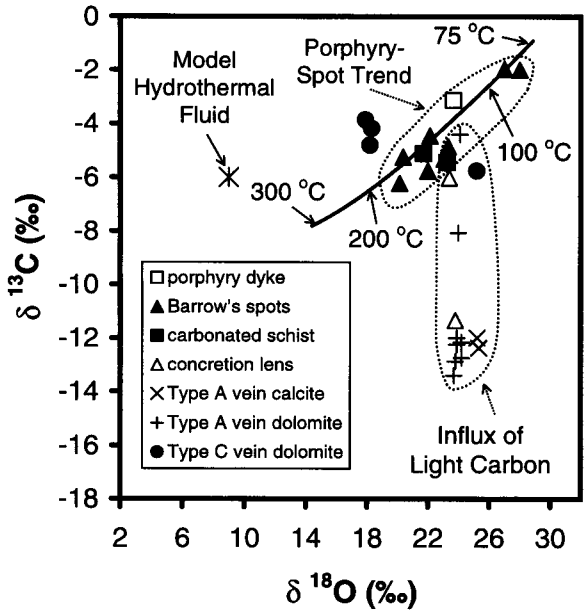

Fig. 5. $\delta^{13}C$–$\delta^{18}O$ plot of post-metamorphic Dalradian-hosted carbonate. Data are fit by a model for the precipitation of calcite from a CO_2 or $H_2CO_{3(aq)}$-bearing hydrothermal fluid of constant isotopic composition ($\delta^{18}O = 9‰$, $\delta^{13}C = -6‰$) over the temperature range 75–200°C. Calcite curve calculated using the fractionation factors of Bottinga (1968) for $\Delta_{CO_2\text{-}CALCITE}$, and O'Neil *et al.* (1969) for $\Delta_{CALCITE\text{-}H_2O}$. The Porphyry-Spot Trend is defined by the data array including carbonate from Barrow's spots, a quartz porphyry dyke, and pervasively carbonated schists. The Influx of Light Carbon field surrounds data from vein dolomite and calcite with low negative $\delta^{13}C$ values, possibly reflecting addition of oxidised organic material to the vein-forming fluid.

boudin-neck veins into the surrounding wallrocks along cleavage surfaces defined by the east-northeast striking regional foliation (strike *c.* 70°; dip *c.* 60°N). In some cases, Type A veins are bounded by selvages containing metamorphic index minerals such as biotite or garnet, implying that they were formed syn-D3 at the latest (Harte *et al.* 1984). Type A veins consist of quartz with inclusions of chlorite ± plagioclase ± dolomite ± calcite ± biotite ± Fe-Ti oxides ± chloritoid. Type A veins within the biotite and garnet zones contain dolomite which clearly crosscuts pre-existing vein quartz, fills in fractures and along grain boundaries, and is undeformed (Fig. 7a). Associated quartz often contains abundant deformation features, including subgrain boundaries, deformation lamellae, and fluid inclusion trails along healed fractures. One sampled Type A vein in the chloritoid zone contains deformed euhedral calcite crystals as much as *c.* 3 cm long. Post-metamorphic carbonate minerals from syn-metamorphic Type A veins have a narrow range of $\delta^{18}O$ values (23.7–25.3‰), but highly variable $\delta^{13}C$ (-13.4 to $-4.4‰$).

Vein Type B, in the chlorite zone, is steeply dipping but strikes at a high angle to regional foliation. The vein studied (strike=357°: dip=82°E) is *c.* 2–3 cm thick and contains two generations of carbonate in addition to quartz and chlorite (Fig. 7b). The first generation consists of cream-coloured calcite that contains abundant deformation twins in thin section and forms bands parallel to the vein margins and concordant with wallrock inclusions and vein quartz (JAB 77A-1; $\delta^{18}O = 11.6‰$ and $\delta^{13}C = -9.0‰$). The second generation of carbonate crosscuts the first generation and is undeformed (JAB 77A-2; $\delta^{18}O = 14.0‰$ and $\delta^{13}C = -5.9‰$).

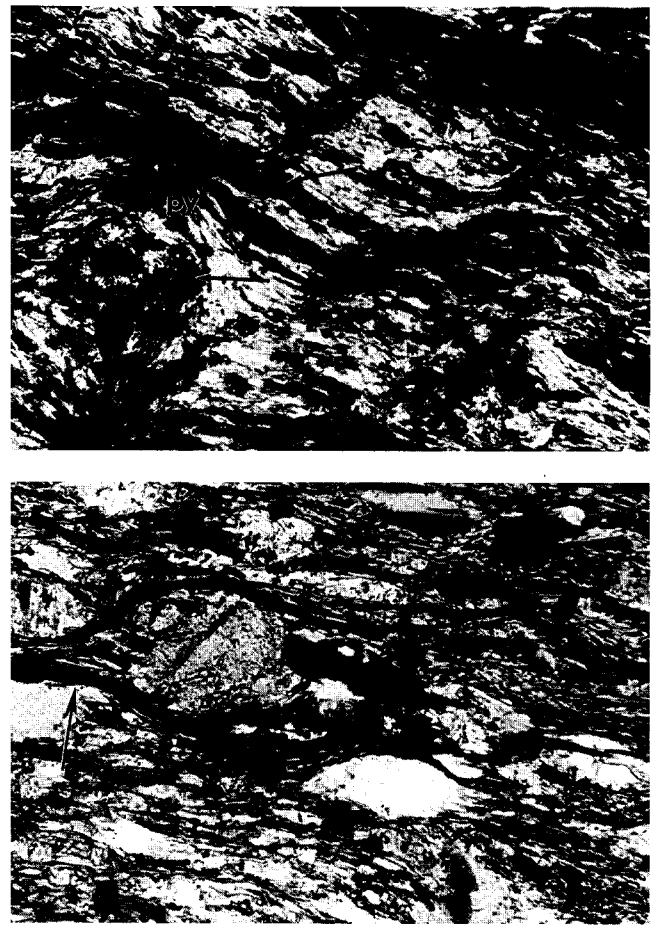

Fig. 6. (**a**) Photomicrograph using plane polarised light of a pervasively carbonated muscovite schist from the biotite zone (JAB 5D). Light coloured patches are muscovite and quartz. Dark zones distributed throughout the photograph (upper arrow points out one example) are siderite. A plagioclase phenocryst has also been altered to siderite (lower arrow). Pyrite is labelled 'py'. Field of view is 1.5 mm across. (**b**) Photomicrograph using plane polarised light of a quartz–muscovite–biotite schist (JAB 3D) from the biotite zone. Siderite in this sample is not as pervasively distributed as in JAB 5D. Siderite is limited to a few millimetre spaced lamellae, parallel to mica-defined schistosity, like that surrounding the large plagioclase phenocryst in the centre-left of the photograph (arrow). Field of view is 1.5 mm across.

Type C veins, from the biotite and garnet zones, crosscut regional foliation at a high angle, consist entirely of carbonate minerals with no evidence of intracrystalline deformation in thin section, and vary between *c.*0.5–2 cm in thickness. Sample JAB 25C, a *c.* 4 mm wide Type C dolomite vein hosted by pervasively carbonated garnet zone schist, has $\delta^{18}O = 25.2‰$ and $\delta^{13}C = -5.7‰$ (Fig. 5). Another Type C vein (JAB 83I A) has similar oscillatory mineralogical zonation to that found in veinlets in the Highland Boundary Fault (JAB 72A; Fig. 3). Dolomite from the vein interior has $\delta^{18}O = 18.2‰$ and $\delta^{13}C = -4.8‰$. Ferruginous dolomite from the vein margins has $\delta^{18}O = 18.1‰$ and $\delta^{13}C = -4.0‰$ (Fig. 5).

Vein quartz

Quartz was collected from Type A and Type B veins (Table 2) directly adjacent to the vein carbonate samples in an attempt

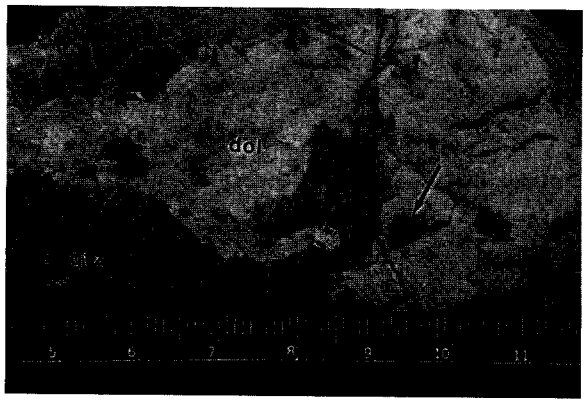

Fig. 7. (**a**) Photograph of carbonate-bearing Type A vein JAB 3A, from the biotite zone, showing vein quartz (qtz) and late vein dolomite (dol). Vein dolomite contains many small vugs (arrow); some are square, suggesting they once contained euhedral pyrite that has since been removed, probably by weathering. Scale is in centimetres. (**b**) Photomicrograph using plane polarised light of Type B vein JAB 77A from the upper chlorite zone. This vein contains at least two generations of calcite (denoted by the numbers in the photograph), quartz (light grey), and chlorite (dark grains in the quartz). Deformed calcite (1), showing deformation twins, has $\delta^{18}O$ values ($\delta^{18}O_{calcite}=11.6‰$) consistent with precipitation of calcite and vein quartz ($\delta^{18}O_{quartz}=13.6‰$) from a single fluid at about 375°C. Undeformed calcite (2) has larger $\delta^{18}O$ values ($\delta^{18}O_{calcite}=13.9‰$) than deformed calcite. A crosscutting veinlet of undeformed calcite (3) may represent a third generation of vein carbonate. Field of view is 2.9 mm across.

to address the degree of isotopic equilibration between vein quartz and carbonate minerals. Quartz from Type A veins has average $\delta^{18}O$ values ranging from 11.7 to 13.2‰. Quartz from the crosscutting Type B vein (JAB 77A) has $\delta^{18}O=13.6‰$.

Discussion

Highland Boundary Fault

Data from samples of Highland Boundary Fault calcite and Fe-dolomite veins and dolomitized spilites fall along a positive trend on a $\delta^{13}C$–$\delta^{18}O$ plot (Fig. 4). We investigate the conditions of carbonate alteration in the Highland Boundary Fault by applying a model for carbonate precipitation from a single fluid over a temperature range to data from the Highland Boundary Fault. The model was developed by Rye & Williams (1981) in the study of hydrothermal dolomite associated with ore-forming fluids in base-metal sulphide deposits. The model uses equations of the form

$$\Delta_{min\text{-}fl}=(A_{min\text{-}fl}\times 10^6)\,T^{-2} \quad (1)$$

where $\Delta_{min\text{-}fl}$ is the equilibrium fractionation between the fluid and the mineral, $A_{min\text{-}fl}$ is the equilibrium $^{18}O/^{16}O$ or $^{13}C/^{12}C$ fractionation coefficient for the fluid relative to the mineral, and T is temperature (K). Equations for oxygen and carbon mineral–fluid isotopic fractionation were used to calculate the isotopic composition of calcite, dolomite and ankerite in equilibrium with the model fluid over a geologically reasonable temperature range. Model calculations produce curves with a positive slope in $\delta^{13}C$–$\delta^{18}O$ space like the trend seen in the Highland Boundary Fault data.

Fractionation factors for calcite and dolomite are relatively well known, but those for ankerite are not. Here, we have used the empirical ankerite–H_2O fractionation equation developed by Mumin *et al.* (1996). For ankerite–CO_2 fractionation, we have used the equation for dolomite–CO_2 fractionation of O'Neil *et al.* (1969), although the actual $\delta^{13}C$ values are likely to be between $\delta^{13}C$ values for the dolomite curve and the siderite curve (Carothers *et al.* 1988).

Fractionation calculations were made with either H_2CO_3 apparent ($H_2CO_{3(ap)}$), CO_2, or HCO_3^- as the dominant carbon species in solution. H_2CO_3 and aqueous CO_2 are often considered together as $H_2CO_{3(ap)}$ because the two species are difficult to distinguish in analytical measurements (Ohmoto & Goldhaber 1997). Fractionation between $H_2CO_{3(ap)}$ and CO_2 above 100°C is considered to be negligible, so the fractionation factors for CO_2 are used to account for both species (Ohmoto 1972). A range of fluid $\delta^{18}O$ and $\delta^{13}C$ compositions were tested using the model equations. Data from both calcite and dolomite are fit by a fluid dominated by $H_2CO_{3(ap)}$ or CO_2 with an isotopic composition of $\delta^{18}O=0‰$ and $\delta^{13}C=-6‰$ over the temperature range 75–150°C (Fig. 4). One sample from a calcite vein in spilitized basalt (JAB 75A-1) does not fall on the trend described above. Calculations using the same model fluid isotopic composition but with HCO_3^- as the dominant carbon-bearing species in solution can account for the outlier vein calcite. The inferred temperature range is consistent with the presence of low temperature mineral assemblages including clay minerals in the altered spilites. Study of fluid inclusions would place additional constraints on the temperature range of alteration, but such an investigation is beyond the scope of this paper.

The fluid composition and temperature range suggested by the model are consistent with carbonation of HBF spilites via hydrothermal seawater circulation. The oxygen isotope value of the model fluid is consistent with that of seawater (Craig 1961), but the carbon isotope value and carbon speciation of the model fluid are not. Dissolved bicarbonate is the dominant carbon-bearing species in seawater and has an average $\delta^{13}C$ value of 0‰, controlled by equilibrium with atmospheric CO_2 (Shanks *et al.* 1995). In the late Cambrian to mid-Ordovician (520–450 Ma), the time frame relevant for this study, seawater $\delta^{13}C$ values were *c.* −1 to −3‰ (Wadleigh & Veizer 1992; Qing & Veizer 1994).

The speciation and isotopic composition of carbon in seawater may be modified by circulation through basalt and seafloor sediments. The dominant carbon-bearing species in solution in ocean-floor hydrothermal vents is CO_2 (Scott 1997). CO_2 in this setting may reflect input from MORB

carbon with isotopic values of $\delta^{13}C_{CO_2} = -3.4$ to -4.1‰ (Gerlach & Taylor 1990) or, where seafloor sediments are present to provide a source of organic carbon, $\delta^{13}C$ values of vent CO_2 can be as low as -10.5‰ (Guaymas Basin, Gulf of California; Peter & Shanks 1992). Hydrothermal seawater circulation modifies the carbon isotopic composition of the fluid to values near that of our model (cf. Scott 1997), values that are essentially an average crustal carbon signature (Ohmoto & Rye 1979).

The $\delta^{18}O$ of the model fluid suggests that the Highland Boundary Fault rocks were altered under high water-rock conditions (Stakes & O'Neil 1982). Seafloor hydrothermal fluids retain the oxygen isotope value of seawater in regions where the water–rock ratio (W/R) is moderate to high (W/R>1; Shanks *et al.* 1995), because seawater is the largest oxygen reservoir in the system. Seawater, however, contains very little carbon (*c.* 0.5 mmol HCO_3^- per kg seawater), so addition of magmatic CO_2 or organic carbon to the hydrothermal fluid would control the carbon isotopic signature of the hydrothermal fluid even at high W/R ratios.

Carbonate alteration due to hydrothermal seawater circulation through basalt, although a common phenomenon (cf. Scott 1997; Stakes & O'Neil 1982), is not necessarily a unique explanation of the Highland Boundary Fault data. At least some of the carbonate minerals in the Highland Boundary Fault may have been precipitated from or equilibrated with an external fluid during emplacement along the fault.

The model for precipitation of carbonate from modified seawater over a temperature range seems to fit the overall coherent trend of the data. However, the scatter of the Highland Boundary Fault dolomite data between the ankerite and dolomite fractionation curves warrants additional discussion. Dolomite iron content is an important factor controlling oxygen isotope fractionation between the mineral and fluid. From the model fractionation curves, the $\delta^{18}O$ ratio of the dolomite becomes more depleted with increasing iron content. Samples closest to the ankerite curve are from pink, ferruginous dolomite veins, while samples closest to the dolomite curve are from pervasively dolomitized spilites. All of the Highland Boundary Fault dolomites probably contain some amount of iron, however, suggesting that the ankerite curve may be more appropriate to use than the pure dolomite curve. Changes in fluid isotopic composition due to fluid-rock interaction along the flow path could also account for the scatter of the data but at present such an interpretation is unconstrained. We conclude that the variable Fe content probably contributes to the scatter evident in Fig. 4.

Syn-metamorphic fluid infiltration: Dalradian

Ague (1997) presented petrochemical evidence for significant fluid infiltration and non-volatile element transport during metamorphism in the chloritoid-bearing rocks within our field area. Carbonate and quartz isotopic data presented here also suggest metamorphic fluid infiltration.

The $\delta^{18}O$ of deformed vein calcite and deformed vein quartz from Type B vein JAB 77A are given in Tables 1 and 2 respectively. JAB 77A is located *c.* 30 m south of the biotite isograd (Fig. 1). Observation of fluid inclusions in the vein minerals suggests that a fluid was present during vein mineral formation. Quartz from JAB 77A has a $\delta^{18}O$ typical of metamorphic quartz (Garlick & Epstein 1967). Fractionation between vein quartz and calcite (Sharp & Kirschner 1994) is consistent with these minerals being precipitated from a single fluid at about 375°C, a temperature consistent with the upper chlorite zone.

Staurolite zone metacarbonate layers have extremely low, negative oxygen and carbon isotope values relative to their probable protolith values. Unmetamorphosed marine limestones have $\delta^{13}C$ and $\delta^{18}O$ values of *c.* 0‰ and *c.* 25‰ respectively (Keith & Weber 1964). Two possible causes of depletion in $\delta^{18}O$ and $\delta^{13}C$ are Rayleigh fractionation of the carbonate or exchange with an external fluid. Rayleigh fractionation calculations (e.g. Lattanzi *et al.* 1980; Nabelek *et al.* 1984) indicate that 98% decarbonation must occur in order to deplete the $\delta^{13}C$ value by 17‰. We have not observed petrographic or structural evidence that suggests such extreme volume loss.

Alternatively, oxygen and carbon depletion in the metacarbonates could have been caused by exchange with an external fluid. The oxygen isotopic composition of such a fluid would reflect the isotopic composition of the bulk rock integrated along the flow path. Quartz is the isotopically heaviest silicate mineral in an equilibrium pelitic assemblage. Typical values of metamorphic quartz from pelitic rocks range from 12–16‰ (Garlick & Epstein 1967), a range including our data from vein quartz. This range is much lower than the bulk $\delta^{18}O$ values of unmetamorphosed limestones (Keith & Weber 1964). The lack of significant amounts of primary carbonate in the Southern Highland Group of the Dalradian suggests that locally or distantly derived metamorphic fluid would be dominated by a silicate isotopic signature, which is consistent with the observed low $\delta^{18}O$ values of the metacarbonates.

The extremely depleted carbon isotope values from these metacarbonate layers suggest that oxidized organic carbon is a possible source for the carbon in the fluid. However, graphite is rare or absent in the rocks of our field area. Organic carbon in the fluids may have been derived from nearly complete oxidation of graphite from local Dalradian metasediments or introduced from some distance away. Graham *et al.* (1983) reached such a conclusion to explain low, negative $\delta^{13}C$ values measured in metacarbonates from the SW Highlands.

Calculations using metacarbonate mineral rim compositions (Table 3) were done to estimate the X_{CO_2} of the fluids in equilibrium with the staurolite zone metacarbonate layers using the TWEEQU program of Berman (1991). The pressure estimate used was 4 kbar (Droop & Harte 1995; Ague 1997). Metamorphic temperature for the staurolite zone was estimated based on Fe-Mg partitioning between coexisting garnet and biotite using TWEEQU (Berman 1991) and the mineral compositions determined by Baltatzis (1979). The two samples of Baltatzis give temperature estimates of 584°C and 604°C. Quartz was assumed to be pure SiO_2. Ideal activity models were used for calcite and clinozoisite (cf. Leger & Ferry 1993), and the activity models recommended by Berman (1991) were used for all other minerals.

Calculations for metacarbonate JAB 109F from the lower staurolite zone used the mineral assemblage calcite+garnet+plagioclase+quartz. The calculated X_{CO_2} ranges between 0.14 and 0.20 for temperatures in the range 584–604°C. Calculations for metacarbonate JAB 15B, also from the staurolite zone, used the mineral assemblage calcite+garnet+clinozoisite+quartz. There is a maximum in the isobaric equilibrium curve for this assemblage at $T=590$°C and $X_{CO_2}=0.82$. The calculated X_{CO_2} is between 0.67 and 0.94 for temperatures above 584°C. X_{CO_2} calculations for these two rocks show that fluid compositions are variable among

Dalradian metacarbonate layers in our field area. The differences in X_{CO_2} between the two layers may be due to differences in reaction history or fluid infiltration history. Investigating the causes of fluid composition differences between the metacarbonate layers is a topic for future research.

Post-metamorphic fluid flow: Dalradian

Isotopic data from the quartz porphyry dyke analysed, pervasively carbonated schists, and Barrow's spots fall along a coherent trend, which we call the porphyry-spot trend (Fig. 5). Isotope data from Type C carbonate veins (JAB 25C and JAB 83I A) and from dolomite from a concretion lens (JAB 3E) in the biotite zone plot near the porphyry-spot trend. The range in $\delta^{18}O$ values for these samples overlaps the range for post-metamorphic vein carbonate from Type A veins and the biotite zone concretions.

The same model for precipitation of calcite from a single fluid over a temperature range constructed for data from the Highland Boundary Fault was applied to the porphyry-spot trend. The data are fit by a fluid dominated by CO_2 or $H_2CO_{3(ap)}$ with an isotopic composition of $\delta^{18}O = 9‰$ and $\delta^{13}C = -6‰$ over the temperature range 75–200°C (Fig. 5). The $\delta^{13}C_{CO_2}$ of this model fluid is identical to the $\delta^{13}C_{CO_2}$ of the Highland Boundary Fault model and is the same as an average crustal carbon composition (Ohmoto & Rye 1979). Unlike the Highland Boundary Fault model fluid, however, the $\delta^{18}O$ of the porphyry-spot fluid suggests a fluid derived from or equilibrated with a high-T silicate reservoir such as felsic igneous rocks or metamorphic rocks.

Hydrothermal circulation systems set up around igneous intrusions commonly cause extensive alteration of the country rock as well as the intrusions themselves, both in the form of pervasive alteration and vein formation (Lowell & Guilbert 1970; Brimhall 1979; So *et al.* 1983; Reed 1994, 1997). Several lines of petrographic evidence suggest that intrusion of the porphyry dykes initiated such a flow regime. For example, the quartz ± kaolinite ± carbonate ± pyrite assemblage, found in the altered dykes, is commonly found in hydrothermal alteration associated with porphyry copper deposits (Reed 1997). In addition to alteration of the dykes, some of the Dalradian metasediments in the surrounding region have been pervasively metasomatised. All these rock types have similar alteration mineral assemblages including carbonates, clays, and sulphides. Carbonates are either disseminated through the schists or are concentrated in closely spaced lamellae (Fig. 6). Other schists in the area that have not been pervasively altered show evidence of localized carbonate addition; for example the original feldspar porphyroblasts of Barrow's spots were commonly modified to carbonate-bearing mineral assemblages. Post-metamorphic Type C carbonate veins containing undeformed dolomite are also found crosscutting schists near the dykes, although a genetic link between these veins and the dykes remains to be established.

Oxygen isotopic evidence also suggests there is a genetic link between carbonate alteration of the Dalradian metasediments and the porphyry dykes. The model fluid is consistent with a fluid from a felsic igneous source (Taylor 1997). Oxygen isotope data suggests that hydrothermal circulation associated with the porphyry dykes may have also been responsible for altering the isotopic composition of the primary carbonate concretion lenses and deposition of carbonate in Type A veins; both sample types have $\delta^{18}O$ values in the middle of the range defined by the porphyry-spot trend.

The isotope data and the field relationships among the various rock types affected by post-metamorphic carbonate alteration suggest that a single fluid infiltration event was responsible for addition of carbonate to the porphyry dykes, pervasively carbonated schists, and Barrow's spots. The dykes are *c.* 15 m thick in outcrop, suggesting that they may be too small to have initiated hydrothermal circulation (Delaney 1987). However, the dykes are only seen in two dimensions on the ground; their three-dimensional geometry is not known and they could be more extensive than is apparent in the field. Furthermore, the dykes are associated with the Younger Granite Series (400–460 Ma, Munro 1986). The granitic bodies could have provided sufficient heat at depth to drive regional hydrothermal circulation.

The isotope systematics do not, however, rule out other retrograde fluid flow events. For example, a fluid equilibrated with Dalradian metasediments at *c.* 500–550°C, such as that produced by metamorphic dehydration, would have $\delta^{18}O$ values *c.* 8–9‰ based on the equilibrium quartz–water fractionation factor of Bottinga & Javoy (1973). If the fluid was cooled to 75–200°C without re-equilibrating with the rocks along the flow path, carbonate minerals precipitated from it would have the observed $\delta^{18}O$ values. Such a scenario, however, does not readily account for the localisation of strong post-metamorphic carbonate alteration in the vicinity of the dykes. Further, it is extremely unlikely that fluids generated at 500°C would be transported to lower temperatures without isotopic exchange with host rocks along the flow path. For example, down temperature channelized fluid flow over a temperature range of 500–200°C, given reasonable flow rates of 10^{-9} to 10^{-11} $m^3\ m^{-2}\ s^{-1}$ and isotopic exchange between the fluid and wallrocks along the flow path, will result in vein minerals becoming isotopically heavier along the flow path (Palin 1992). For fluids generated from Dalradian metasediments under metamorphic conditions (500°C) and a reasonable geothermal gradient to cool to <200°C without any exchange would require unreasonably fast rates of channelised fluid flow over a *c.* 10 km scale flow path.

The carbon isotopic composition of the model fluid is indistinguishable from average crustal carbon (Ohmoto & Rye 1979). Carbon isotopes from concretion lenses from the biotite zone and Type A veins, however, require a more depleted fluid. For example, concretion lenses have $\delta^{13}C$ values that are *c.* 3–8‰ lower than the porphyry-spot trend, while Type A veins have extremely variable negative $\delta^{13}C$ values, as much as 10‰ lighter than the trend. The isotopically light carbon signature of these samples could be accounted for by variable addition of carbon from an organic source over a restricted time period during the history of the hydrothermal circulation system because oxidised organic carbon typically has $\delta^{13}C$ values *c.* −25‰ (Ohmoto & Rye 1979). The source of organic carbon is unconstrained by our data. Primary organic carbon in the form of graphite is rare in the rocks of this part of the Dalradian. Organic carbon in the fluid may have been derived from nearly complete oxidation of graphite from local Dalradian metasediments or introduced from some external source.

Petrographic observations and isotopic evidence suggest that Type A veins originally formed during metamorphism (cf. Ague 1997). For example, the quartz oxygen isotopic data from these veins (Table 2) are typical for metamorphic quartz (Garlick & Epstein 1967). Comparison of isotopic data from vein quartz and vein dolomite reveals extreme isotopic disequilibrium between the two minerals. Equilibrium fractionation between quartz and dolomite is at most *c.* 1‰ over the

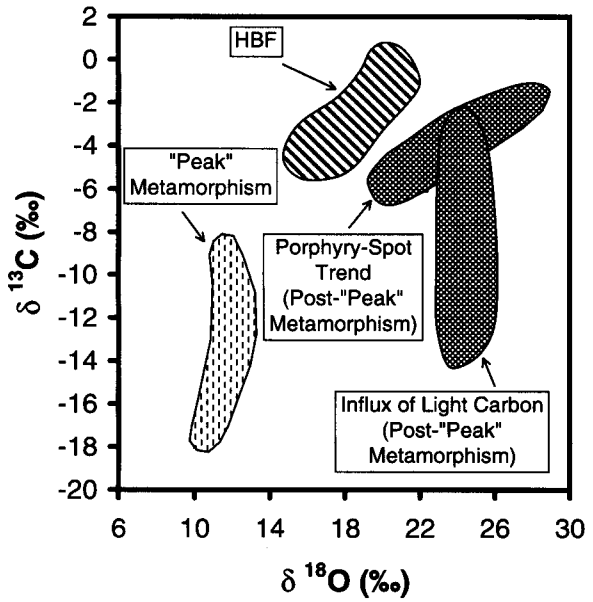

Fig. 8. $\delta^{13}C$–$\delta^{18}O$ plot of data fields discussed in the text. The 'HBF' field corresponds to the field defined in Fig. 4 for data from the Highland Boundary Fault. The Porphyry-Spot Trend (Post-'Peak' Metamorphism) and Influx of Light Carbon (Post-'Peak' Metamorphism) fields correspond to the Porphyry-Spot Trend and Influx of Light Carbon fields in Fig. 5. Data from staurolite zone metacarbonates (JAB 109 and JAB 15) and syn-metamorphic vein calcite (JAB 77A-1) from the chlorite zone are included in the 'Peak'-Metamorphism field.

geologically reasonable temperature range 300–600°C (Northrop & Clayton 1966; Bottinga & Javoy 1973), while the difference between measured quartz and dolomite from Type A veins is greater than 10‰. The isotopic data are consistent with the petrographic observations suggesting that the dolomite is a post-metamorphic addition to these veins (Fig. 7a). An important implication of these data is that fluids associated with retrograde circulation reused metamorphic fracture networks during post-metamorphic fluid infiltration.

Summary and conclusions

We have presented petrographic evidence and stable isotopic measurements from 35 hand samples that suggests the Highland Border Complex and the Dalradian metasediments north of Stonehaven, Scotland have been affected by multiple episodes of fluid-rock interaction. The fields defined by the isotopic data are presented in Fig. 8 for comparison.

The Dalradian metasediments have been affected by both syn-metamorphic and post-metamorphic fluid infiltration (Fig. 8). Carbon and oxygen isotopes in staurolite zone metacarbonate layers ($\delta^{18}O_{calcite}$=10.4 to 12.9‰, $\delta^{13}C_{calcite}$= − 12.4 to − 17.7‰) have been significantly depleted relative to their probable protolith values (Fig. 8; 'Peak' Metamorphism). Rayleigh fractionation during decarbonatization cannot explain such extreme depletion of $\delta^{13}C$ values. However, the oxygen isotope data are consistent with depletion due to infiltration of the metacarbonates by a fluid in equilibrium with a silicate reservoir at metamorphic temperatures, probably from surrounding metapelitic and metapsammitic rocks. Oxidized organic carbon in the infiltrating fluid, perhaps introduced from oxidation of graphite now rare in the Dalradian, could explain the carbon isotope depletion. Calcite and quartz from a vein in the chlorite zone have isotopic values ($\delta^{18}O_{calcite}$=11.6‰; $\delta^{18}O_{quartz}$=13.6‰) consistent with precipitation from a metamorphic fluid at *c.* 375°C.

Petrographic and isotopic evidence from spatially related alteration in a variety of rock types including sedimentary concretion lenses, veins, Devonian-aged quartz porphyry dykes, and schists, including Barrow's spotted schists, suggests that post-metamorphic fluid infiltration was regionally widespread and was responsible for carbonate addition to these rock types (Fig. 8; Porphyry-Spot Trend (Post-'Peak' Metamorphism)). Isotopic data are consistent with precipitation of carbonate minerals from low-temperature fluids (75–200°C) that were originally equilibrated with a high-temperature silicate reservoir. Precipitation probably occurred during circulation of hydrothermal fluids around the quartz porphyry dykes. Pervasive fluid flow was responsible for extensive carbonate addition in the dykes and surrounding schists. Channelized flow deposited dolomite in post-metamorphic carbonate veins and reused old metamorphic fracture networks, depositing post-metamorphic dolomite or calcite in syn-metamorphic quartz veins. Post-metamorphic carbonate in syn-metamorphic quartz veins records the presence of light carbon in the fluid ($\delta^{13}C$= − 8.1 to − 13.4‰), perhaps reflecting oxidation of organic matter in the Dalradian metasediments (Fig. 8; Influx of Light Carbon (Post-'Peak' Metamorphism)).

Petrographic and isotopic evidence suggests that the Highland Border Complex has been affected by fluid infiltration. Spilites from a dismembered ophiolite in the Highland Boundary Fault were altered by hydrothermal circulation on the sea floor or during emplacement in the fault. Spilites have been pervasively altered to dolomite and ferruginous dolomite, probably at relatively low temperatures in the range 75–150°C, by a fluid with an oxygen isotopic composition consistent with seawater ($\delta^{18}O \approx 0$‰) but with a carbon isotopic composition ($\delta^{13}C$= − 6‰) modified by addition of magmatic carbon or oxidised organic material (Fig. 8, 'HBF').

Financial support from National Science Foundation grant EAR-9405889 is gratefully acknowledged. Careful reviews by C. Graham and G. Jenkin greatly improved the manuscript. We would like to thank J. Kingston and J. Eckert for their excellent scientific and technical assistance.

References

AGUE, J.J. 1997. Crustal mass transfer and index mineral growth in Barrow's garnet zone, northeast Scotland. *Geology*, **25**, 73–76.

ANDERSON, J.G.C. 1947. The geology of the Highland Border: Stonehaven to Arran. *Transactions of the Royal Society of Edinburgh*, **61**, 479–515.

ATHERTON, M.P. 1977. The metamorphism of the Dalradian rocks of Scotland. *Scottish Journal of Geology*, **13**, 331–370.

BALTATZIS, E. 1979. Staurolite-forming reactions in the eastern Dalradian rocks of Scotland. *Contributions to Mineralogy and Petrology*, **69**, 193–200.

BARROW, G. 1893. On an intrusion of muscovite biotite gniess in the southeast Highlands of Scotland and its accompanying metamorphism. *Quarterly Journal of the Geological Society of London*, **49**, 330–358.

—— 1898. Chloritoid schists from Kincardineshire. *Quarterly Journal of the Geological Society of London*, **54**, 149–155.

—— 1912. On the geology of the lower Deeside and the Southern Highland Border. *Proceedings of the Geologists' Association*, **23**, 268–273.

BERMAN, R.G. 1991. Thermobarometry using multi-equilibrium calculations: A new technique, with petrological applications. *Canadian Mineralogist*, **29**, 833–855.

BOTTINGA, Y. 1968. Calculation of fractionation factors for carbon and oxygen exchange in the system calcite-carbon dioxide-water. *Journal of Physical Chemistry*, **72**, 800–808.

—— & JAVOY, M. 1973. Comments on oxygen isotope geothermometry. *Earth and Planetary Science Letters,* **20,** 250–265.

BRIMHALL, G.H. 1979. Lithologic determination of mass transfer mechanisms of multiple-stage porphyry copper mineralization at Butte, Montana; vein formation by hypogene leaching and enrichment of potassium-silicon protore. *Economic Geology,* **74,** 556–589.

CAROTHERS, W.W., ADAMI, L.H. & ROSENBAUER, R.J. 1988. Experimental oxygen isotope fractionation between siderite-water and phosphoric acid liberated CO_2-siderite. *Geochimica et Cosmochimica Acta,* **52,** 2445–2450.

CHINNER, G.A. 1966. The distribution of pressure and temperature during Dalradian metamorphism. *Quarterly Journal of the Geological Society of London,* **122,** 159–186.

—— 1967. Chloritoid and the isochemical character of Barrow's zones. *Journal of Petrology,* **8,** 268–282.

CLAYTON, R.N. & MAYEDA, T.K. 1963. The use of bromine pentafluoride in the extraction of oxygen from oxides and silicates for oxygen isotopic analyses. *Geochimica et Cosmochimica Acta,* **27,** 43–52.

COLE, C. & GRAHAM, C. 1994. Stable isotope and textural evidence on the mechanisms of metamorphic fluid infiltraion within a zone of structurally-focused high fluid flux. *Mineralogical Magazine,* **58A,** 187–188.

CRAIG, H. 1961. Isotopic variations in meteoric waters. *Science,* **133,** 1702–1703.

CRAW, D. 1990. Regional fluid and metal mobility in the Dalradian metamorphic belt, Southern Grampian Highlands, Scotland. *Mineralium Deposita,* **25,** 281–288.

DELANEY, P.T. 1987. Heat transfer during emplacement and cooling of mafic dykes. *In*: HALLS, H.C. & FAHRIG, W.F. (eds) *Mafic dyke swarms.* Geological Association of Canada Special Papers, **34,** 31–46.

DROOP, G.T.R. & HARTE, B. 1995. The effect of Mn on the phase relations of medium-grade pelites. *Journal of Petrology,* **36,** 1549–1578.

FEIN, J.B., GRAHAM, C.M., HOLNESS, M.B., FALLICK, A.E. & SKELTON, A.D.L. 1994. Controls on the mechanisms of fluid infiltration and front advection during regional metamorphism: a stable isotope and textural study of retrograde Dalradian rocks of the SW Scottish Highlands. *Journal of Metamorphic Geology,* **12,** 249–260.

FETTES, D.J. 1979. A metamorphic map of the British and Irish Caledonides. *In*: HARRIS, A.L., HOLLAND, C.H. & LEAKE, B.E. (eds) *The Caledonides of the British Isles—reviewed.* Geological Society, London, Special Publications, **8,** 307–321.

FETTES, D.J., GRAHAM, C.M., HARTE, B. & PLANT, J.A. 1986. Lineaments and basement domains: and alternative view of Dalradian evolution. *Journal of the Geological Society, London,* **143,** 453–464.

GARLICK, G.D. & EPSTEIN, S. 1967. Oxygen isotope ratios in coexisting minerals of regionally metamorphosed rocks. *Geochimica et Cosmochimica Acta,* **31,** 181–214.

GERLACH, T.M. & TAYLOR, B.E. 1990. Carbon isotope constraints on degassing of carbon dioxide from Kilauea volcano. *Geochimica et Cosmochimica Acta,* **54,** 2051–2058.

GRAHAM, C.M., GREIG, K.M., SHEPPARD, S.M.F. & TURI, B. 1983. Genesis and mobility of the H_2O-CO_2 fluid phase during regional greenschist and epidote amphibolite facies metamorphism: a petrological and stable isotope study in the Scottish Dalradian. *Journal of the Geological Society, London,* **140,** 577–599.

GRAHAM, C.M., SKELTON, A.D.L., BICKLE, M. & COLE, C. 1997. Lithological, structural, and deformation controls on fluid flow during regional metamorphism. *In*: HOLNESS, M.B. (ed.) *Deformation-enhanced Fluid Transport in the Earth's Crust and Mantle.* Chapman & Hall, London, 196–226.

HARRIS, A.L. & PITCHER, W.S. 1975. The Dalradian Supergroup. *In*: HARRIS, A.L. *ET AL.* (eds) *A Correlation of the Precambrian Rocks of the British Isles.* Geological Society, London, Special Reports, **6,** 52–75.

——, BRADBURY, H.J. & MCGONIGAL. 1976. The evolution and transport of the Tay Nappe. *Scottish Journal of Geology,* **12,** 103–113.

HARTE, B. 1988. Lower Paleozoic metamorphism in the Moine-Dalradian belt of the British Isles. *In*: HARRIS, A.L. & FETTES, D.J. (eds) *The Caledonian–Appalachian Orogen.* Geological Society, London, Special Publications, **38,** 123–134.

——, BOOTH, J.E., DEMPSTER, T.J., FETTES, D.J., MENDUM, J.R. & WATTS, D. 1984. Aspects of the post-depositional evolution of Dalradian and Highland Boundary rocks in the Southern Highlands of Scotland. *Transactions of the Royal Society of Edinburgh, Earth Sciences,* **75,** 151–163.

HENDERSON, W.G. & ROBERTSON, A.H.F. 1982. The Highland Border rocks and their relation to marginal basin development on the Scottish Caledonides. *Journal of the Geological Society, London,* **139,** 433–450.

HUTTON, D.H.W. 1987. Strike-slip terranes and a model for the evolution of the British and Irish Caledonides. *Geological Magazine,* **124,** 405–425.

IKIN, N.P. & HARMON, R.S. 1983. A stable isotope study of serpentinization and metamorphism in the Highland Border Suite, Scotland, U.K. *Geochimica et Cosmochimica Acta,* **47,** 153–167.

JENKIN, G.R.T., FALLICK, A.E. & LEAKE, B.E. 1992. A stable isotope study of retrograde alteration in SW Connemara, Ireland. *Contributions to Mineralogy Petrology,* **110,** 269–288.

KEITH, M.L. & WEBER, J.W. 1964. Carbon and oxygen isotopic composition of selected limestones and fossils. *Geochimica et Cosmochimica Acta,* **28,** 1787–1816.

LATTANZI, P., RYE, D.M. & RICE, J.M. 1980. Behavior of 13C and 18O in carbonates during contact metamorphism at Marysville, Montana; implications for isotope systematics in impure dolomitic limestones. *American Journal of Science,* **280,** 890–906.

LEGER, A. & FERRY, J.M. 1993. Fluid infiltration and regional metamorphism of the Waits River Formation, North-east Vermont, USA. *Journal of Metamorphic Geology,* **11,** 3–29.

LOWELL, J.D. & GUILBERT, J.M. 1970. Lateral and vertical alteration-mineralization zoning in porphyry copper deposits. *Economic Geology,* **65,** 373–408.

MUMIN, A.H., FLEET, M.E. & LONGSTAFFE, F.J. 1996. Evolution of hydrothermal fluids in the Ashanti Gold Belt, Ghana: stable isotope geochemistry of carbonates, graphite, and quartz. *Economic Geology,* **91,** 135–148.

MUNRO, M. 1986. *Geology of the country around Aberdeen: Memoir for 1:50 000 sheet 77 (Scotland).* British Geological Survey, London.

NABELEK, P.I., LABOTKA, T.C., O'NEIL, J.R. & PAPIKE, J.J. 1984. Continuous fluid/rock interaction between the Notch Peak granitic intrusion and argillites and limestones in western Utah: evidence from stable isotopes and phase assemblages. *Contributions to Mineralogy Petrology,* **86,** 25–34.

NORTHROP, D.A. & CLAYTON, R.N. 1966. Oxygen-isotope fractionations in systems containing dolomite. *Journal of Geology,* **74,** 174–196.

OHMOTO, H. 1972. Systematics of sulfur and carbon isotopes in hydrothermal ore deposits. *Economic Geology,* **67,** 551–579.

—— & GOLDHABER, M.B. 1997. Sulfur and carbon isotopes. *In*: BARNES, H.L. (ed.) *Geochemistry of Hydrothermal Ore Deposits,* 3rd edition, John Wiley & Son, New York, 517–612.

—— & RYE, R.O. 1979. Isotopes of sulfur and carbon. *In*: BARNES, H.L. (ed.) *Geochemistry of Hydrothermal Ore Deposits.* 2nd Edition, John Wiley & Son, New York, 509–567.

O'NEIL, J.R., CLAYTON, R.N. & MAYEDA, T.K. 1969. Oxygen isotope fractionation in divalent metal carbonates. *Journal of Chemical Physics,* **51,** 5547–5558.

PALIN, J.M. 1992. *Petrologic and Stable Isotopic Studies of Wepawaug Schist, Connecticut.* PhD Thesis, Yale University.

PETER, J.M. & SHANKS, W.C. III. 1992. Sulfur, carbon, and oxygen isotope variations in submarine hydrothermal deposits of Guaymas Basin, Gulf of California. *Geochimica et Cosmochimica Acta,* **56,** 2025–2040.

QING, H. & VEIZER, J. 1994. Oxygen and carbon isotopic composition of Ordovician brachiopods: Implications for coeval seawater. *Geochimica et Cosmochimica Acta,* **58,** 4429–4442.

REED, M.H. 1994. Hydrothermal alteration in active continental hydrothermal systems. *In*: LENTZ, D.R. (ed.) *Alteration and Alteration Processes Associated with Ore-Forming Systems.* Geological Association of Canada, Short Course Notes, **11,** 315–337.

—— 1997. Hydrothermal alteration and its relationship to ore fluid composition. *In*: BARNES, H.L. (ed.) *Geochemistry of Hydrothermal Ore Deposits,* 3rd Edition, John Wiley & Son, New York, 303–366.

ROBERTSON, A.H.F. & HENDERSON, W.G. 1984. Geochemical evidence for the origins of igneous and sedimentary rocks of the Highland border, Scotland. *Transactions of the Royal Society of Edinburgh,* **75,** 135–150.

ROGERS, G., DEMPSTER, T.J., BLUCK, B.J. & TANNER, P.W.G. 1989. A high-precision U-Pb age for the Ben Vuirich granite: implications for the evolution of the Scottish Dalradian Supergroup. *Journal of the Geological Society, London,* **146,** 789–798.

RYAN, P.D., SOPER, N.J., SNYDER, D.B., ENGLAND, R.W. & HUTTON, D.H.W. 1995. The Antrim–Galway Line: a resolution of the Highland Border Fault enigma of the Caledonides of Britain and Ireland. *Geological Magazine,* **132,** 171–184.

RYE, R.O. 1993. The evolution of magmatic fluids in the epithermal environment: the stable isotope perspective. *Economic Geology,* **88,** 733–753.

RYE, D.M. & WILLIAMS, N. 1981. Studies of the base metal sulfide deposits at McArthur River, Northern Territory, Australia: III. The stable isotope geochemistry of the H.Y.C., Ridge, and Cooley Deposits. *Economic Geology,* **76,** 1–26.

SCOTT, S.D. 1997. Submarine hydrothermal systems and deposits. *In*: BARNES, H.L. (ed.) *Geochemistry of Hydrothermal Ore Deposits,* 3rd Edition, John Wiley & Son, New York, 797–876.

SHACKLETON, R.M. 1958. Downward facing structures of the Highland Border. *Quarterly Journal of the Geological Society, London,* **113,** 361–392.

SHANKS, W.C. III, BOHLKE, J.K. & SEAL, R.R.II. 1995. Stable isotopes in mid-ocean ridge hydrothermal systems: interactions between fluids, minerals, and organisms. *In*: BARNES, H.L. (ed.) *Seafloor Hydrothermal Systems: Physical, Chemical, Biological, and Geological Interactions.* AGU Geophysical Monographs, **91,** 194–221.

SHARP, Z.D. & KIRSCHNER, D.L. 1994. Quartz-calcite oxygen isotope thermometry: A calibration based on natural isotopic variations. *Geochimica et Cosmochimica Acta,* **58,** 4491–4501.

SKELTON, A.D.L., GRAHAM, C.M. & BICKLE, M.J. 1995. Lithological and structural controls on regional 3-D fluid flow patterns during greenschist facies metamorphism of the Dalradian of the SW Scottish Highlands. *Journal of Petrology,* **36,** 563–586.

SO, C.S., RYE, D.M. & SHELTON, K.L. 1983. Carbon, hydrogen, oxygen, and sulfur isotope and fluid inclusion study of the Weolag tungsten-molybdenum deposit, Republic of Korea: Fluid histories of metamorphic and ore-forming events. *Economic Geology,* **78,** 1551–1573.

STAKES, D.S. & O'NEIL, J.R. 1982. Mineralogy and stable isotope geochemistry of hydrothermally altered oceanic rocks. *Earth and Planetary Science Letters,* **57,** 285–304.

SWART, P.K., BURNS, S.J. & LEDER, J.J. 1991. Fractionation of the stable isotopes of oxygen and carbon in carbon dioxide during the reaction of calcite with phosphoric acid as a function of temperature and technique. *Chemical Geology,* **86,** 89–96.

TANNER, P.W.G. 1995. New evidence that the Lower Cambrian Leny Limestone at Callander, Perthshire, belongs to the Dalradian Supergroup, a reassessment of the "exotic" status of the Highland Border Complex. *Geological Magazine,* **132,** 473–483.

TAYLOR, H.P. 1974. The application of oxygen and hydrogen isotope studies to problems of hydrothermal alteration and ore deposition. *Economic Geology,* **69,** 843–883.

—— 1997. Oxygen and hydrogen isotope relationships in hydrothermal mineral deposits. *In*: BARNES, H.L. (ed.) *Geochemistry of Hydrothermal Ore Deposits,* 3rd Edition, John Wiley & Son, New York, 229–302.

TILLEY, C.E. 1924. The facies classification of metamorphic rocks. *Geological Magazine,* **61,** 167–171.

—— 1925. A preliminary survey of metamorphic zones in the southern Highlands of Scotland. *Quarterly Journal of the Geological Society of London,* **81,** 100–112.

WADLEIGH, M.A. & VEIZER, J. 1992. $^{18}O/^{16}O$ and $^{13}C/^{12}C$ in lower Paleozoic articulate brachiopods: Implications for the isotopic composition of seawater. *Geochimica et Cosmochimica Acta,* **56,** 431–443.

YARDLEY, B.W.D. & BALTATZIS, E. 1985. Retrogression of staurolite schists and the sources of infiltrating fluids during metamorphism. *Contributions to Mineralogy Petrology,* **89,** 59–68.

—— & BOTTRELL, S.H. 1992. Silica mobility and fluid movement during metamorphism of the Connemara schists, Ireland. *Journal of Metamorphic Geology,* **10,** 453–464.

Received 12 October 1998; revised typescript accepted 23 June 1999.
Scientific editing by Ray Burgess.